

Multitaper Array Processing

Kathleen E. Wage

November 2007

*Proceedings of the 41st Asilomar Conference on Signals, Systems, and
Computers, pp. 1242-1246*

© 2007 IEEE. Personal use of this material is permitted. However, permission to reprint/republish this material for advertising or promotional purposes or for creating new collective works for resale or redistribution to servers or lists, or to reuse any copyrighted component of this work in other works must be obtained from the IEEE.

Multitaper Array Processing

Kathleen E. Wage

Department of Electrical and Computer Engineering

George Mason University

4400 University Drive, MSN 1G5

Fairfax, VA 22030-4444, USA

kwage@gmu.edu

Abstract—Thomson’s multitaper approach generates estimates of the power spectrum by averaging individual “eigenspectra” obtained using a set of orthogonal window functions. The multitaper method is designed to work with very low sample support, typically a single snapshot of data, making it very attractive for the analysis of nonstationary or transient signals. This paper explores the use of the multitaper approach for spatial spectrum estimation in passive sonar. Several examples are given, and the problem of processing non-planewave signals is briefly discussed using an example motivated by a deep water propagation experiment.

I. INTRODUCTION

Adaptive array processing algorithms facilitate the detection and localization of quiet sources by nulling out noise and interference. Most adaptive processors rely on time averages to generate the statistics (usually a sample covariance matrix) required for weight vector calculations. When the inputs are non-stationary, the processor has fewer time snapshots to work with, and the result is often substantial degradation in performance. Low sample support is a significant problem for the large aperture arrays currently used in passive sonar [1]. The signals recorded on arrays in the ocean can be non-stationary for a variety of reasons, including source and/or receiver motion, environmental fluctuations, and transient excitation of sources.

The multitaper method, formulated by Thomson for non-parametric spectral estimation [2], is designed to work with low sample support. Multitaper estimates are often formed using a single snapshot of data. Thomson’s basic idea is to apply a set of orthonormal tapers (windows) to the data and then average the spectra obtained with these windows. Averaging over different tapers reduces the variance of the spectral estimate, in the same way that averaging over snapshots in the conventional Welch-Bartlett approach [3] reduces the variance.

While the multitaper method has been used extensively in geophysical time series analysis, very few researchers have applied it to the spatial spectral estimation problem. Drosopoulous and Haykin used a multitaper approach to solve a low-angle tracking radar problem [4]. In a series of papers Clark, Scharf, and Mullis investigated quadratic estimators of the frequency-wavenumber spectrum, including a multidimensional version

of the Thomson estimator [5], [6], [7]. Liu and Van Veen combined the multitaper method with the minimum variance method [8]. Their approach requires estimation of a covariance matrix, thus it requires more snapshots than the standard multitaper implementation. Onn and Steinhardt considered the problem of detecting a sinusoid at a known frequency and unknown direction of arrival using a small set of sensors [9].

This paper investigates the application of multitaper method to the passive sonar problem. The following section presents a framework for multitaper array processing and discusses the detection of planewave components. Section III describes the performance of the multitaper processor using several examples, including one that illustrates the problem of processing non-planewave signals. Section IV concludes the paper.

II. MULTITAPER ARRAY PROCESSING FRAMEWORK

In addition to Thomson’s seminal paper from 1982, a number of other sources describe the multitaper method. The textbook by Percival and Walden is an excellent introduction to multitaper spectral estimation [10]. The book chapter by Drosopoulous and Haykin provides a tutorial on using multitaper methods for radar applications [4]. For a condensed overview of the multitaper method, see the recent article by Thomson [11].

A. Beamspace interpretation of a multitaper processor

From an array processing perspective, the multitaper approach consists of a beamspace processor followed by a weighted averaging operation. Figure 1 shows a basic framework for multitaper processing of narrowband sonar receptions. First, the data is passed through a processor that projects the data into several orthogonal beams centered around the angle of interest θ . The beamspace is defined by the set of orthogonal weight vectors contained in the matrix \mathbf{W} . The k th weight vector is the array response vector $\mathbf{v}(\theta)$ multiplied by a window (taper) \mathbf{u}_k , *i.e.*,

$$\mathbf{w}_k(\theta) = \mathbf{u}_k \odot \mathbf{v}(\theta), \quad (1)$$

where \odot represents the Hadamard product (element-wise multiplication) of the two vectors. The columns of \mathbf{W} are orthogonal, assuming that the set of tapers are chosen to be orthogonal. Thomson suggests using the discrete prolate

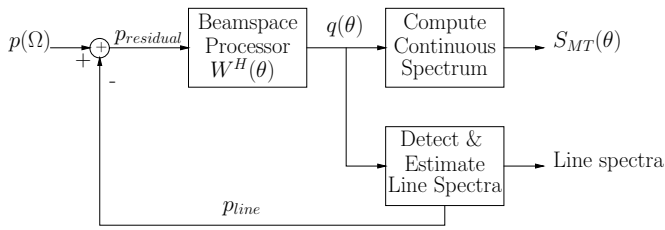


Fig. 1. Multitaper array processing framework. The multitaper approach projects the narrowband pressure field data into an orthogonal beamspace and computes the spectral estimate by averaging over the beam outputs. An iterative algorithm is used to remove planewave (line) components.

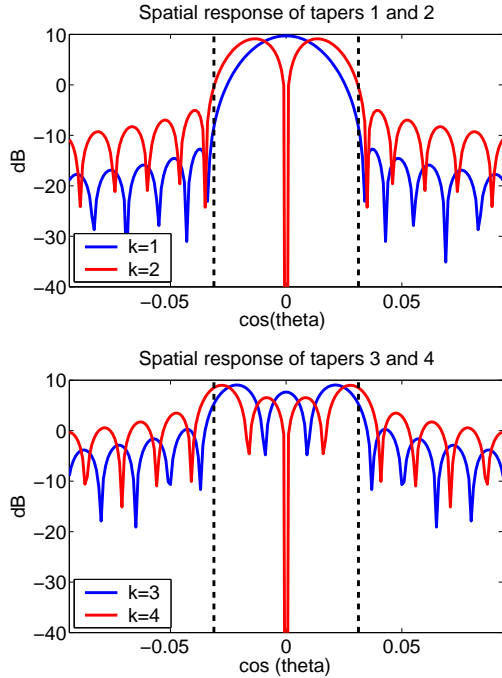


Fig. 2. Beam response (spatial frequency response) of four discrete prolate spheroidal sequence tapers as a function of the cosine of the angle. The tapers are designed for a 128-element equally-spaced array.

spheroidal sequences (DPSS) since they are designed to maximize the power concentrated in a narrow angular region. Figure 2 shows the beam response (spatial frequency response) of a set of four DPSS tapers as a function of the cosine of the angle. The dashed lines in the plots indicate the width of the angular region the tapers are designed to sample. Given a desired beamwidth, the number of tapers guaranteed to have good sidelobe characteristics is limited, thus the multitaper approach uses only these tapers.

The output of the narrowband beamspace processor designed with K tapers is the K -dimensional vector \mathbf{q} :

$$\mathbf{q}(\theta, \Omega) = \mathbf{W}^H(\theta)\mathbf{p}(\Omega). \quad (2)$$

To compute an estimate of the spatial spectrum, the multitaper processor averages the outputs of the beamspace processor,

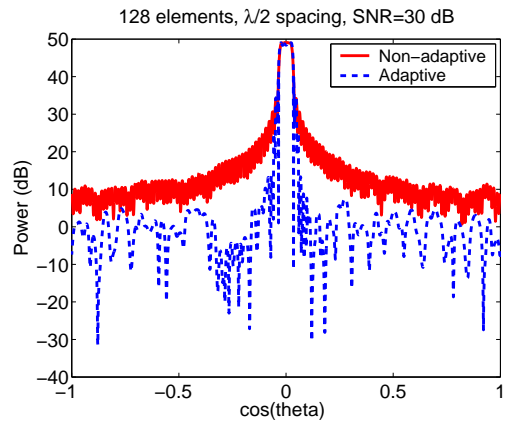


Fig. 3. Multitaper spatial spectrum for a planewave at broadside ($u=0$) with SNR of 30 dB estimated using a 128-element array with half-wavelength spacing. The plot compares the non-adaptive and adaptive multitaper estimators.

i.e., the estimate is

$$S_{MT}(\theta) = \sum_{k=1}^K \alpha_k |q_k(\theta)|^2, \quad (3)$$

where α_k is the weight given to the k th beam output. The weights can be set to $\frac{1}{K}$ for a simple average or determined adaptively. See Thomson's paper [2] for an explanation of the adaptive weight calculation. Figure 3 compares the output of the non-adaptive and adaptive multitaper estimators for an environment containing a single planewave source at broadside in a background of white sensor noise. The array has 128 elements with half-wavelength spacing, and the estimate was generated using the four DPSS tapers shown above. Note that choosing the beamwidth of the multitaper processor requires a tradeoff of resolution and variance, *i.e.*, using a large number of tapers yields a significant reduction in variance with a corresponding reduction in resolution. Figure 3 illustrates how the adaptive weighting can significantly reduce the sidelobes associated with a loud source by applying a data-dependent weighting to the tapered spectral estimates.

B. Detection of planewave components

Equation 3 provides an estimate of the continuous spatial spectrum, but as Thomson suggests, line components need to be estimated separately. In the passive sonar problem, line components correspond to planewave arrivals. These can be estimated using a linear regression on the output of the beamspace processor. Drosopoulos and Haykin discuss the detection of line components in detail for a radar problem [4]. To work with sonar data, where the signal is typically modeled as complex Gaussian, these techniques must be extended. The CFAR subspace detection scheme developed by Jin and Friedlander provides a useful framework for analyzing and implementing planewave detectors [12].

Consider a received signal consisting of a single planewave plus noise:

$$\mathbf{p} = \tilde{\mathbf{b}}\mathbf{v}(\theta) + \mathbf{n}. \quad (4)$$

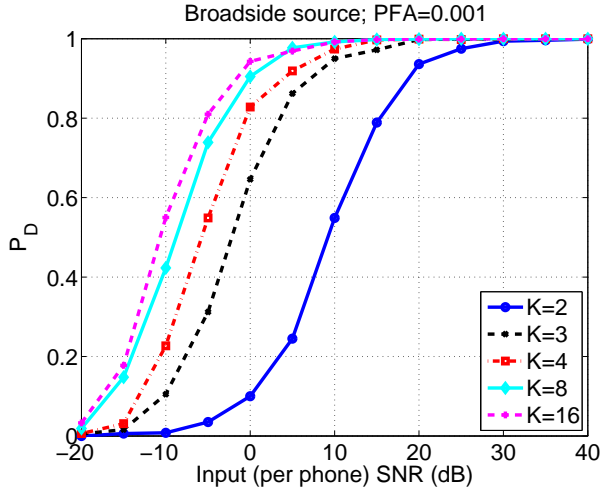


Fig. 4. Detection performance as a function of SNR and the number of tapers. Results shown are for a 128-element array with half-wavelength spacing. The detector uses a single snapshot and the false alarm probability is fixed at 0.001.

The output of the k th filter steered towards θ is:

$$q_k(\theta) = \mathbf{w}_k^H(\theta)\mathbf{p} = \tilde{b}\mu_k + \mathbf{w}_k^H(\theta)\mathbf{n}, \quad (5)$$

where μ_k is the DC component of the k th taper:

$$\mu_k = \sum_{n=1}^N u_k(n). \quad (6)$$

In this case the output of the beamspace processor is

$$\mathbf{q}(\theta) = \mathbf{W}_{\text{beam}}^H(\theta)\mathbf{p} = \tilde{b}\boldsymbol{\mu} + \text{noise}.$$

Linear regression yields a simple estimate of the complex amplitude \tilde{b} :

$$\hat{b}(\theta) = (\boldsymbol{\mu}^H \boldsymbol{\mu})^{-1} \boldsymbol{\mu}^H \mathbf{q}(\theta). \quad (7)$$

Based on Jin and Friedlander's results, a CFAR statistic for detecting the presence of a single planewave in noise is

$$\frac{\mathbf{q}^H \mathbf{P}_\mu \mathbf{q}}{\mathbf{q}^H \mathbf{P}_{\text{orth}} \mathbf{q}} \sim \text{F statistic}, \quad (8)$$

where \mathbf{P}_μ is the projection matrix for the subspace spanned by the vector $\boldsymbol{\mu}$ and \mathbf{P}_{orth} represents the projection into the orthogonal subspace: $\mathbf{P}_{\text{orth}} = \mathbf{I} - \mathbf{P}_\mu$. If additional data are available, the test statistic can be averaged over L snapshots:

$$\frac{\sum_l \mathbf{q}_l^H \mathbf{P}_\mu \mathbf{q}_l}{\sum_l \mathbf{q}_l^H \mathbf{P}_{\text{orth}} \mathbf{q}_l}. \quad (9)$$

Figure 4 shows the probability of detection P_D versus SNR for a false alarm rate of 0.001 and varying numbers of tapers. Note that for this single planewave case, increasing the number of tapers improves P_D up to a point. Beyond eight tapers, performance doesn't improve much since the higher tapers do not sample the center of the band (the angle associated with the planewave) very well.

An iterative scheme is useful for detecting low-level planewave components in the presence of loud interferers. As

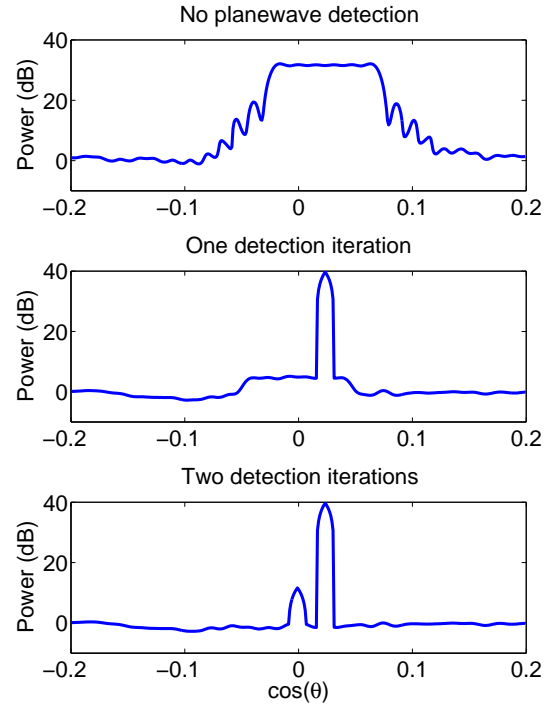


Fig. 5. Example of iterative detection of planewave components. The plots show results for a 128-element array with half-wavelength spacing. Two planewaves with SNR's of 20 dB and -10 dB relative to the white noise floor are incident on the array. With no planewave detection, the output spectrum is the blurred peak shown in the top plot. The results of the first detection iteration (shown in the middle plot) indicate that the strong planewave is detected. After the second detection iteration (bottom plot), both planewaves are visible.

shown in Figure 1, the planewave signals are estimated and removed after one pass through the beamspace processor. The residual signal is fed back through the beamspace processor again, and the planewave detection/estimation algorithm is repeated. Figure 5 illustrates the output of the multitaper processor after each iteration when the input signal consists of two closely-spaced planewaves. For this simulation the array has 128 elements with half-wavelength spacing. The two sources have different power levels: the first has 20 dB signal-to-noise ratio (SNR) with respect to the white noise floor and the second has -10 dB SNR with respect to the noise floor. As Figure 5 shows, when no planewave detection is implemented, the sources appear as a blurred peak in the output spectrum. After the first iteration, the strong source is detected, but the weak source still appears to be blurred. After the second iteration, both the strong and weak sources are clearly visible in the output.

III. EXAMPLES

This section compares the performance of the multitaper processor to a standard adaptive beamformer, and briefly discusses the modifications necessary to process non-planewave signals.

A. Multitaper versus Minimum Power Distortionless Response

Figure 6 compares the performance of the multitaper processor with the performance of the standard minimum power distortionless response (MPDR) processor for a complicated simulation example. The MPDR weight vector is defined as

$$\mathbf{w}_{\text{MPDR}}(\theta) = \frac{\hat{\mathbf{R}}^{-1}\mathbf{v}(\theta)}{\mathbf{v}(\theta)^H \hat{\mathbf{R}}^{-1}\mathbf{v}(\theta)}. \quad (10)$$

$\hat{\mathbf{R}}$ is the sample covariance matrix of the received pressure

$$\hat{\mathbf{R}} = \sum_{l=1}^L \mathbf{p}_l \mathbf{p}_l^H + \gamma \mathbf{I}, \quad (11)$$

where \mathbf{p}_l is the l th data snapshot and γ is an optional diagonal loading parameter (needed to stabilize the inverse). See the text by Van Trees for a thorough description of the MPDR approach [13].

In this example, the array consists of 128 elements with half-wavelength spacing. The environment contains one moving source and 13 stationary interferers. The moving source has a -10 dB SNR with respect to the white noise floor; the stationary interferers have varying power levels. Note that the interferers located near endfire (four near forward endfire and four near aft endfire) are perfectly coherent. Each processor uses 4 snapshots to compute its estimates. The MPDR processor requires diagonal loading to stabilize the inversion of its sample covariance matrix¹. Figure 6 shows that the multitaper processor produces spatial spectra with significantly lower variance than the MPDR processor. As a result the low-level moving source is easier to see in the multitaper output than it is in the MPDR output. In addition, the multitaper processor handles the coherent sources without a problem, whereas the MPDR processor nulls out some of the coherent signal components. While forward-backward averaging can help the MPDR processor with coherent sources, this would require additional computation that the multitaper approach does not require. As Figure 6 illustrates, the multitaper processor performs very well for a long array using only a few snapshots.

B. Application of multitapering to non-planewave sources

In some underwater environments the arriving signal is better described as a sum of the propagating modes of the waveguide than as a sum of planewaves. Consider a simulation example motivated by the SPICE04 experiment [14]². The top plot in Figure 7 shows the reception at 1000 km range due to a transient source with a center frequency of 250 Hz. As is typical in deep water, the early-arriving energy corresponds to the higher modes and the late-arriving energy corresponds to the lower modes. The lower plot in Figure 7 shows the planewave detection statistic for the multitaper processor designed for the 250 Hz bin. Based on this plot, the early part

¹A reasonable loading level was used; no attempt was made to optimize the choice of loading level.

²The array configuration for the simulation does not match the SPICE04 experiment exactly. Specifically, the sensor spacing for the simulation has been adjusted to half-wavelength to eliminate grating lobes.

of the arrival pattern consists of the sum of two planewaves whose angle changes as a function of time. This is consistent with the WKB approximation, which says a mode can be thought of as the sum of an up- and a down-going planewave (see Figure 8 showing the shape of mode 40 as a function of depth). While WKB theory works well for the higher order modes, it typically breaks down for the lower modes, which is why the multitaper display for the later part of the arrival pattern is more difficult to interpret. Since the low modes cannot be written as the sum of up/down-going planewaves, the multitaper detector must be modified to accurately detect these signals.

IV. SUMMARY

This paper applied Thomson's multitaper method to the passive sonar problem. As the example in Section III-A demonstrated, the multitaper processor can reliably detect low-level planewave arrivals in a complicated background containing coherent and incoherent interference sources. Additional work is ongoing to adapt the multitaper method to process non-planewave signals, such as those recorded during SPICE04.

REFERENCES

- [1] A. B. Baggeroer and H. Cox, "Passive Sonar Limits Upon Nulling Multiple Moving Ships with Large Aperture Arrays," in *Proceedings of the 33rd Asilomar Conference on Signals, Systems, and Computers*, pp. 103–108, 1999.
- [2] D. J. Thomson, "Spectrum estimation and harmonic analysis," *Proceedings of the IEEE*, vol. 70, pp. 1055–1096, September 1982.
- [3] P. Welch, "The use of the Fast Fourier Transform for the estimation of power spectra," *IEEE Trans. on Audio and Electroacoustics*, vol. AU-15, pp. 70–73, June 1967.
- [4] A. Drosopoulos and S. Haykin, "Adaptive radar parameter estimation with Thomson's multiple window method," in *Adaptive Radar Detection and Estimation*, New York, NY: John Wiley, 1991.
- [5] M. P. Clark, L. L. Scharf, and C. T. Mullis, "Quadratic estimators of the frequency-wavenumber spectrum," in *Proceedings of the International Conference on Acoustics, Speech, and Signal Processing*, vol. 4, pp. 2329–2332, April 1991.
- [6] M. P. Clark and L. L. Scharf, "Frequency-wavenumber spectrum analysis using quadratic estimators," in *Proceedings of the 6th SP Workshop on Statistical Signal and Array Processing*, pp. 416–419, October 1992.
- [7] M. P. Clark and L. L. Scharf, "Efficient frequency-wavenumber spectrum estimation using sliding time-division windows," in *Proceedings of the 26th Asilomar Conference on Signals, Systems, and Computers*, pp. 1116–1121, October 1992.
- [8] T.-C. Liu and B. D. V. Veen, "Multiple Window Based Minimum Variance Spectrum Estimation for Multidimensional Random Fields," *IEEE Trans. on Signal Processing*, vol. 40, pp. 578–589, March 1992.
- [9] R. Onn and A. O. Steinhardt, "A multiwindow method for spectrum estimation and sinusoid detection in an array environment," *IEEE Trans. on Signal Processing*, vol. 42, pp. 3006–3015, November 1994.
- [10] D. B. Percival and A. T. Walden, *Spectral Analysis for Physical Applications: Multitaper and Conventional Univariate Techniques*. Cambridge University Press, 1993.
- [11] D. J. Thomson, "Jackknifing multitaper spectrum estimates," *IEEE Signal Processing Magazine*, vol. 24, pp. 20–30, July 2007.
- [12] Y. Jin and B. Friedlander, "A CFAR adaptive subspace detector for second-order gaussian signals," *IEEE Trans. on Signal Processing*, vol. 53, pp. 871–884, March 2005.
- [13] H. L. Van Trees, *Optimum Array Processing*. New York, NY: John Wiley and Sons, 2002.
- [14] P. F. Worcester, M. A. Dzieciuch, L. J. V. Uffelen, D. L. Rudnick, B. D. Cornuelle, and W. H. Munk, "The SPICEX (Spice Experiment) component of the 2004 North Pacific Acoustic Laboratory (NPAL) experiment: An overview," in *J. of the Acoustical Society of America*, vol. 120, p. 3020, November 2006.

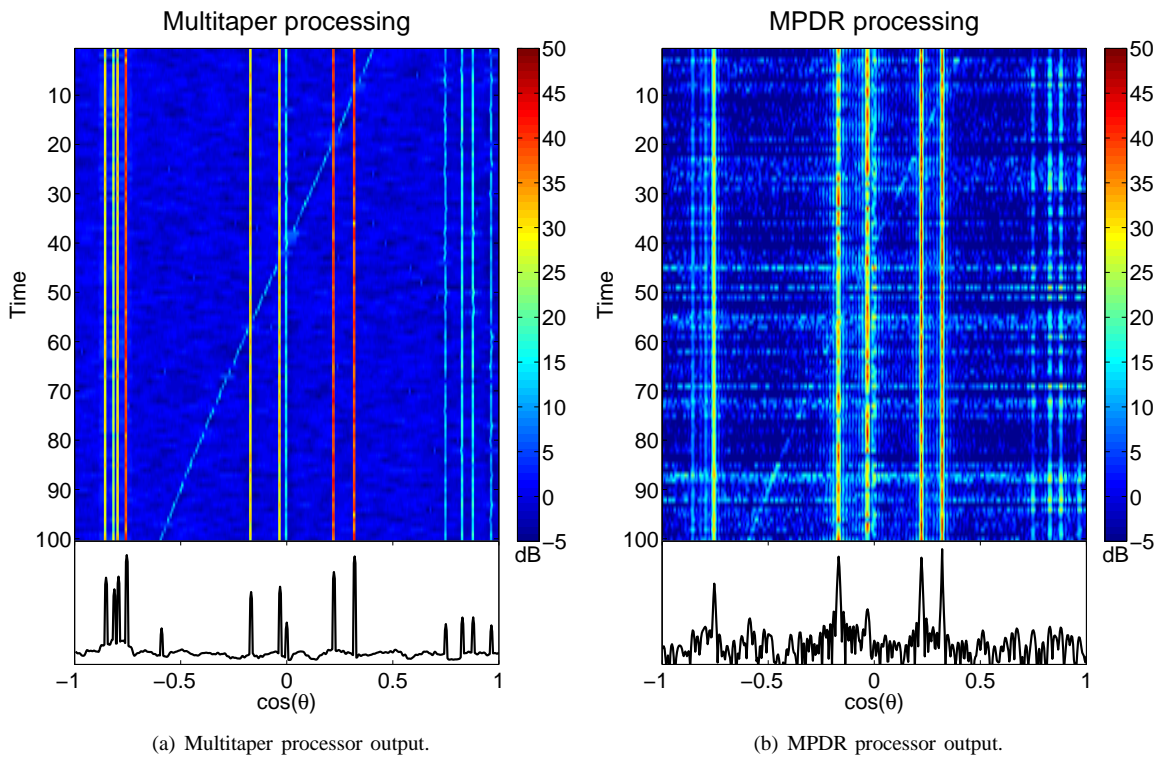


Fig. 6. Comparison of the outputs of narrowband multitaper and minimum power distortionless response processors for a complicated scenario containing one moving source and 13 stationary interferers. The array consists of 128 elements with half-wavelength spacing. The color images show the estimated spatial spectra for 100 different trials, and the line plots at the bottom of each figure show the results for the 100th trial.

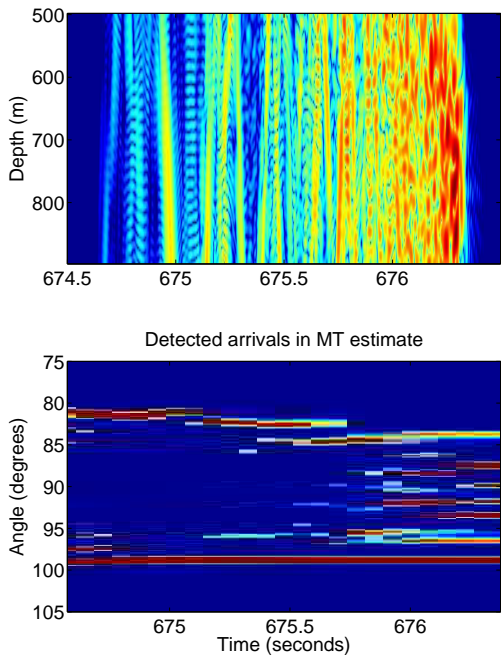


Fig. 7. Simulation motivated by the SPICE04 experiment. The top plot shows the received pressure field at a range of 1000 km for a transient source centered at 250 Hz.

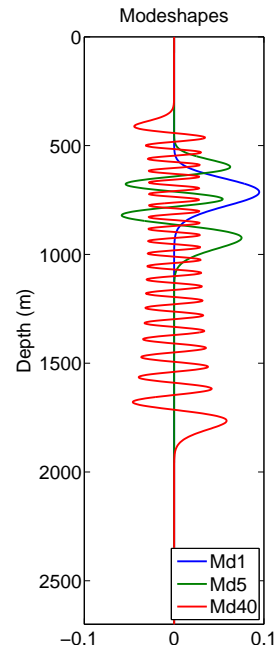


Fig. 8. Modeshapes for modes 1, 5, and 40 at 250 Hz for the SPICE04 simulation environment.